AIP | Applied Physics Letters

An electrospun fiber phototransistor by the conjugated polymer poly[2-methoxy-5-(2'-ethylhexyloxy)-1,4-phenylene-vinylene]

Deyu Tu, Stefano Pagliara, Roberto Cingolani, and Dario Pisignano

Citation: Applied Physics Letters **98**, 023307 (2011); doi: 10.1063/1.3534803
View online: http://dx.doi.org/10.1063/1.3534803
View Table of Contents: http://scitation.aip.org/content/aip/journal/apl/98/2?ver=pdfcov
Published by the AIP Publishing

An electrospun fiber phototransistor by the conjugated polymer poly[2-methoxy-5-(2'-ethylhexyloxy)-1,4-phenylene-vinylene]

Deyu Tu,[1] Stefano Pagliara,[1] Roberto Cingolani,[2] and Dario Pisignano[1,3,a)]
[1]*NNL, National Nanotechnology Laboratory of Istituto Nanoscienze-Consiglio Nazionale delle Ricerche, via Arnesano, I-73100 Lecce, Italy*
[2]*Italian Institute of Technology (IIT), via Morego 30, I-16163 Genova, Italy*
[3]*Dipartimento di Ingegneria dell'Innovazione, Università del Salento, via Arnesano, I-73100 Lecce, Italy*

(Received 1 September 2010; accepted 16 December 2010; published online 14 January 2011)

We investigate the photoresponse of field-effect transistors based on conjugated polymer electrospun fibers. The electrical performances of single fiber transistors are controlled by modulating the channel conductivity under white light illumination. We demonstrate a photoresponsivity up to 100 mA/W for a 500-nm channel width fiber phototransistor illuminated by an intensity of 9.6 mW/cm^2. Studying the photoresponse switching cycles evidences that the photocurrent relaxation time can be reduced down to about 40 s by increasing the fiber surface-to-volume ratio. © *2011 American Institute of Physics*. [doi:10.1063/1.3534803]

Optoelectronic devices based on conjugated polymers attract attention because of their tunability, flexibility, and low cost, which make them ideal for large-area, lightweight and foldable products, and compatible with plastic substrates.[1–3] Polymer thin films are widely exploited in light-emitting diodes,[4] field-effect transistors (FETs),[3] solar cells,[5] photodetectors,[6] and phototransistors.[7,8] In particular, phototransistors, whose output current depends on both photoinduced and gate-induced carriers,[9] show high sensitivity and low noise,[10] and, since combining light detection and electrical signal magnification in a single device, are expected to be key components of future optoelectronic integration systems.[7,10]

A challenge of thin film phototransistors made by conjugated polymers, such as polythiophene, polyphenylene vinylene (PPV), and some of their derivatives,[11–13] is the persistent photocurrent after the termination of illumination, which strongly limits the operation speed. Such a behavior is related to the dispersive diffusion either of photogenerated bipolarons to the surface, where dissociation, polaron transport, and recombination take place,[14] or of positive polarons created by pairs dissociation through interaction with oxygenated defects.[15] Investigating this issue is particularly fascinating for PPV-derivatives as the poly[2-methoxy-5-(2'-ethylhexyloxy)-1,4-phenylene-vinylene] (MEH-PPV),[11] shows good stability in air,[16] excellent luminescence,[4] and possibility to be processed and patterned into one-dimensional (1D) fiber nanostructures.[17] However, while inorganic nanowires, carbon nanotubes, and small-molecule micro/nanoribbons are already exploited in phototransistors,[10,18–20] the photoresponse of conjugated polymer 1D nanostructures has been mainly explored by two-terminal measurements.[21–23]

A very effective route to embed conjugated polymer nanostructures in optoelectronic devices is represented by electrospinning (ES),[23–26] which is a simple, cheap, and high-throughput technology relying on the uniaxial elongation of a polymer solution jet under an applied electric field.[27] ES allows to control the diameter of active polymer fibers from a few micrometers down to tens of nanometers by optimizing the process parameters.[17,28–30] In this letter, we study the photocurrent in single MEH-PPV fiber phototransistors by varying the fiber dimension and thus the phototransistor channel width. Bottom-contact, back-gated fiber devices with 500-nm channel width exhibit photocurrent/dark current ratio (P) and responsivity (R) up to 10 and up to 100 mA/W, respectively. In addition, the photocurrent decay is studied, for which we find that the relaxation time can be reduced down to about 40 s by increasing the fiber surface-to-volume ratio.

Our devices are realized on single-side polished n-type silicon (100) wafers (resistivity <6 mΩ·cm), coated by a thermally grown, 400 nm SiO_2 layer (Silicon Materials, Landsberg am Lech, Germany). 2×2 mm^2 source and drain electrodes (Cr/Au with thickness 5/50 nm, respectively) with gap of 15 μm or 19 μm are defined by photolithography, metal physical vapor deposition, and lift-off. A layer of hexamethyldisilazane is spin-cast on samples to optimize the dielectric-organics interface.[24] 8–27 μM chloroform solutions of MEH-PPV (Sigma-Aldrich, St. Louis, bottom inset of Fig. 1) are used for ES because of their good processability[24] and electrical performances.[31] 400–600 μl of the polymer solution are stored in a 1.0 ml syringe tipped with a 27-gauge stainless steel needle, and injected at the end of the needle at a rate of 10–20 μl/min by a syringe pump. The positive lead of a high voltage supply (5–15 kV) is

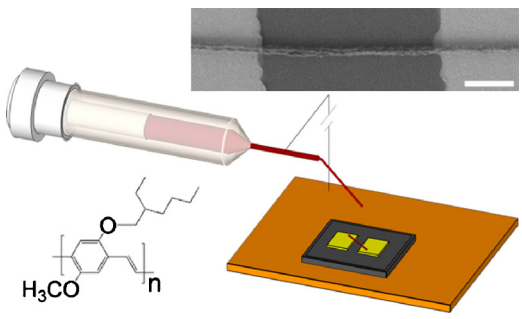

FIG. 1. (Color online) Schematics of ES process to fabricate single fiber phototransistors. Bottom inset: MEH-PPV molecular structure. Top inset: SEM micrographs of a typical device ($L=19$ μm, $W=0.5$ μm). Bar $=5$ μm.

a)Author to whom correspondence should be addressed. Electronic mail: dario.pisignano@unisalento.it.

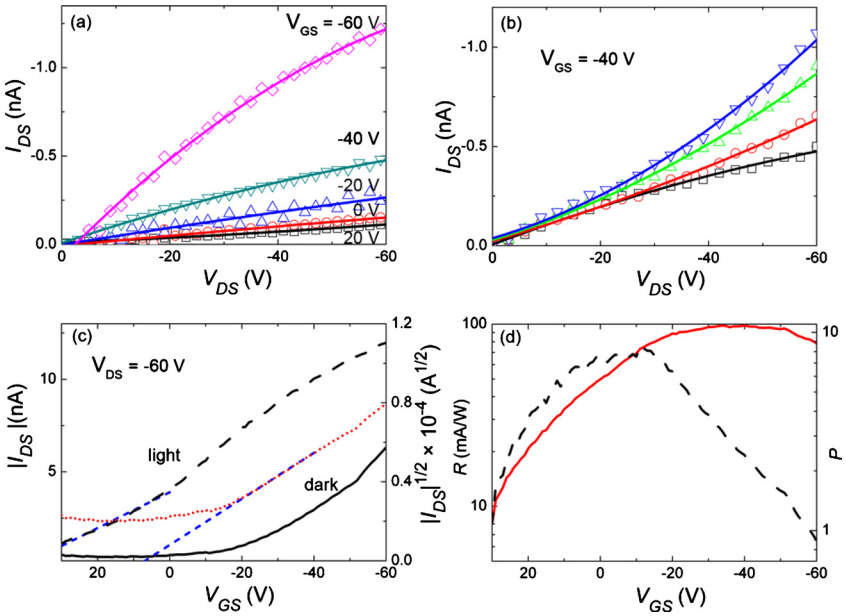

FIG. 2. (Color online) (a) Output characteristics of a single MEH-PPV fiber phototransistor (L=15 μm, W=0.5 μm). I_{DS} vs V_{DS} curves for V_{GS}=0 V (squares), −10 V (circles), −20 V (upward triangles), −40 V (downward triangles), and −60 V (diamonds). Superimposed curves are best fits by FET characteristics. (b) Current-voltage characteristics at V_{GS}=−40 V. P_{in}=0 (squares), 0.1 (circles), 1.2 (upward triangles), and 9.6 mW/cm^2 (downward triangles). (c) Transfer characteristic ($|I_{DS}|$ vs V_{GS}, left scale) in dark (solid line) and under irradiation (long-dashed line) with P_{in} =9.6 mW/cm^2 for V_{DS}=−60 V. $|I_{DS}|$ vs V_{GS} (right scale, dotted line). The short-dashed curves are linear fit to data in the saturation (for device in dark) and linear region (for device under irradiation), respectively. (d) P (dashed line, right vertical scale) and R (solid line, left scale) vs V_{GS}. (P_{in}=9.6 mW/cm^2, V_{DS}=−60V).

connected to the metal needle, and the Si substrates with the Cr/Au electrodes are placed on a Cu collector biased at −6 kV, at about 10 cm from the syringe (Fig. 1). A scanning electron microscopy (SEM) image of a single fiber MEH-PPV phototransistor with channel length (L) of 19.0 μm and width (W) of 0.5 μm is displayed in the top inset of Fig. 1. The devices are finally annealed in N_2 to remove residual solvent and enhance adhesion on the dielectric surface. A probe station and a stereomicroscope (Stemi DV4, Carl Zeiss MicroImaging GmbH, Standort Göttingen—Vertrieb, Germany) are used for contacting the device. The electrical characterization is carried out in air at room temperature and in dark by a semiconductor parameter analyzer (4200 SCS, Keithley, Cleveland). Broad-band white light is provided by the stereomicroscope illuminator, and photoresponse switching cycles are carried out with light duration around 10 s, each cycle being defined as the lapse of time between turning on irradiation and photocurrent decay to the initial state after stopping irradiation.

For gate voltages (V_{GS}) decreasing from 20 to −60 V in the dark, the drain current (I_{DS}) dependence on the drain voltage (V_{DS}) highlights a p-type behavior of the transistor, working in accumulation mode [Fig. 2(a)]. Figure 2(b) shows instead the current-voltage characteristics (at V_{GS}=−40 V) under light intensity (P_{in}) varying from 0 to 9.6 mW/cm^2. The channel current increases correspondingly,[32] resembling the field effect of Fig. 2(a), though without reaching saturation as also reported for organic single-crystalline submicrometer ribbons.[10]

Figure 2(c) displays the transfer characteristics, $I_{DS}(V_{GS})$, at V_{DS}=−60 V, collected in the dark and under irradiation. These characteristics are typically analyzed by modifying the traditional FET model to include bulk linear effects enhanced under illumination:[12] $I_{DS}=I_{Ch}+I_{\text{bulk}}=C\mu W[(V_{GS}-V_{TH})V_{DS}-V_{DS}^2/2]/2L+Ne\mu WTV_{DS}/L$, where I_{Ch} and I_{bulk} indicate injected and photogenerated current, respectively, C is the capacitance per unit area of the dielectric material, μ the mobility of the majority carriers, V_{TH} the threshold bias, N the charge density in the bulk, and T the thickness of the deposited fiber. In the dark, the onset of the saturation is appreciable, where $I_{DS}=C\mu W(V_{GS}-V_{TH})^2/2L$. The saturation mobility, in the dark, and the linear mobility, under irradiation, are calculated to be 9.4×10^{-4} and 6.7×10^{-4} cm^2/V s, respectively [Fig. 2(c)], with on-off switching current ratio, $I_{\text{on}}/I_{\text{off}}$=21(11), and V_{TH}=8(40)V, under dark (illumination) conditions, respectively. The lower μ and $I_{\text{on}}/I_{\text{off}}$ observed under irradiation are due to the enhancement of the carrier density which mainly affects the device off-state.[33] The concomitant large variation of V_{TH} is due to both (i) the photogenerated electrons accumulating under the source and lowering the source-channel potential barrier thus enhancing I_{Ch} and (ii) the higher density of the carriers outside the channel due to photogeneration, which increases I_{bulk}, as found in MEH-PPV film phototransistors.[7]

The photosensitivity, $P=(I_{DS}^{\text{light}}-I_{DS}^{\text{dark}})/I_{DS}^{\text{dark}}$,[34] is up to about 10 (with P_{in}=9.6 mW/cm^2). This value is comparable or higher with respect to previous reports of single 1D conjugated polymer nanostructure photodetectors,[22,21] though still at least one order of magnitude lower than those of thin film polymer phototransistors.[7,32,35] The dependence of P on V_{GS} is shown in Fig. 2(d) (dashed curve). For $|V_{GS}|$ well-above threshold, the current weakly increases under illumination, leading to P around 1 at a gate voltage of −60 V. Instead, the current below or slightly above threshold significantly increases and the maximum $P(\sim10)$ is reached at V_{GS}=−10 V.

To better compare the optical response of devices of different channel width, we determine the responsivity R defined as $(I_{DS}^{\text{light}}-I_{DS}^{\text{dark}})/P_{in}LW$. For P_{in}=9.6 mW/cm^2 and V_{DS}=−60 V, R is maximum in the strong-accumulation regime [up to 100 mA/W for $V_{GS}<-50$ V, Fig. 2(d)]. As for other organic phototransistors,[34] this finding indicates a gain effect, as the density of photogenerated carriers per se is expected to depend mainly on P_{in}, and not on V_{GS}. Responsivity values of the order of 100 mA/W are well into the range typical of conjugated polymer phototransistors which span from tens of A/W to fraction of mA/W for devices illuminated by resonantly matching the polymer absorption spectrum[8,32,35] and by broad-band light,[33,34] respectively.

Finally, the photoresponse cycles for single-fiber devices with different channel width in the range of 0.5–80 μm are displayed in Fig. 3. The decrease of the

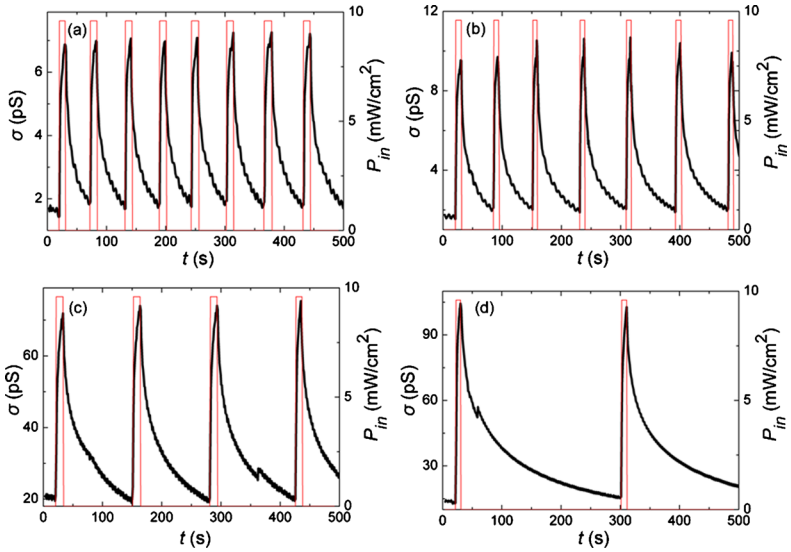

FIG. 3. (Color online) Photoconductivity cycles (V_{DS}=−50 V, V_{GS}=0 V). Transistor channel width =0.5 (a), 5 (b), 40 (c), and 80 μm (d).

photoinduced conductivity (σ) after the termination of illumination is well described by a stretched-exponential,[14,15] $\sigma(t)=\sigma_0 \exp[-(t/\tau)^{\beta}]$, where σ_0 is the initial photoconductivity, τ is the relaxation time, and $0<\beta<1$, highlighting the presence of a distribution of decay-times. We find that the mean relaxation time decreases from about 140 to about 40 s by scaling down the transistor channel width. The long-lasting tail of the photocurrent can be related to slow dispersive diffusion of polaron species to the surface of the organic material[14] or to oxygenated defects.[15,36] Such reacting sites may be randomly distributed, with higher density expected for fibers with higher surface-to-volume ratio, as we observe in light-emitting nanofibers quenched during ultraviolet excitation.[29] Assuming that recombination takes place only near the surface and that diffusional processes follow random paths at a constant speed, v, i.e., with the longest path of diffusion being from the fiber axis to the furthest surface edge, one would expect a decay-time roughly in inverse proportion to the surface-to-volume ratio, with a residual relaxation (in the scale of seconds to tens of seconds) still present for very small nanofiber diameters. The long-lasting tail of the photocurrent in the conjugated polymer may be suppressed by realizing and characterizing fibers under vacuum or controlled atmosphere, thus leading the photocurrent to a regime dominated by fast intrinsic components, generally attributed to the kinetics of the exciton dissociation[15] or of the recombination of free polarons (P^+) in reaction sites with larger recombination rate constant than oxygenated defects.[36]

We acknowledge the financial support from the Italian Minister of University and Research (FIRB RBFR08DJZI "Futuro in Ricerca").

[1]D. H. Park, M. S. Kim, and J. Joo, Chem. Soc. Rev. **39**, 2439 (2010).
[2]H. Klauk, *Organic Electronics* (Wiley, Weinheim, 2006).
[3]J. Zaumseil and H. Sirringhaus, Chem. Rev. **107**, 1296 (2007).
[4]R. H. Friend, R. W. Gymer, A. B. Holmes, J. H. Burroughes, R. N. Marks, C. Taliani, D. D. C. Bradley, D. A. Dos Santos, J. L. Brédas, M. Lögdlund, and W. R. Salaneck, Nature (London) **397**, 121 (1999).
[5]B. H. Hamadani, S. Jung, P. M. Haney, L. J. Richter, and N. B. Zhitenev, Nano Lett. **10**, 1611 (2010).
[6]X. Gong, M. Tong, Y. Xia, W. Cai, J. S. Moon, Y. Cao, G. Yu, C.-L. Shieh, B. Nilsson, and A. J. Heeger, Science **325**, 1665 (2009).
[7]Y. R. Liu, J. B. Peng, and P. T. Lai, Thin Solid Films **516**, 4295 (2008).
[8]X. Wang, K. Wasapinyokul, W. De Tan, R. Rawcliffe, A. J. Campbell, and D. D. C. Bradley, J. Appl. Phys. **107**, 024509 (2010).
[9]S. M. Sze, *Physics of Semiconductor Devices* (Wiley, New York, 1981), chap. 14.
[10]Q. Tang, L. Li, Y. Song, Y. Liu, H. Li, W. Xu, Y. Liu, W. Hu, and D. Zhu, Adv. Mater. **19**, 2624 (2007).
[11]K. W. Lee, K. H. Mo, I.-m Kim, and C. E. Lee, Solid State Commun. **136**, 63 (2005).
[12]S. Dutta and K. S. Narayan, Phys. Rev. B **68**, 125208 (2003).
[13]S. Dutta and K. S. Narayan, Adv. Mater. **16**, 2151 (2004).
[14]C. H. Lee, G. Yu, and A. J. Heeger, Phys. Rev. B **47**, 15543 (1993).
[15]B. Dulieu, J. Wéry, S. Lefrant, and J. Bullot, Phys. Rev. B **57**, 9118 (1998).
[16]A. J. J. M. van Breemen, P. T. Herwig, C. H. T. Chlon, J. Sweelssen, H. F. M. Schoo, E. M. Benito, D. M. de Leeuw, C. Tanase, J. Wildeman, and P. W. M. Blom, Adv. Funct. Mater. **15**, 872 (2005).
[17]F. Di Benedetto, A. Camposeo, S. Pagliara, E. Mele, L. Persano, R. Stabile, R. Cingolani, and D. Pisignano, Nat. Nanotechnol. **3**, 614 (2008).
[18]S. Han, W. Jin, D. Zhang, T. Tang, C. Li, X. Liu, Z. Liu, B. Lei, and C. Zhou, Chem. Phys. Lett. **389**, 176 (2004).
[19]M. Freitag, Y. Martin, J. A. Misewich, R. Martel, and Ph. Avouris, Nano Lett. **3**, 1067 (2003).
[20]Y. Guo, C. Du, G. Yu, C. Di, S. Jiang, H. Xi, J. Zheng, S. Yan, C. Yu, W. Hu, and Y. Liu, Adv. Funct. Mater. **20**, 1019 (2010).
[21]G. A. O'Brien, A. J. Quinn, D. A. Tanner, and G. Redmond, Adv. Mater. **18**, 2379 (2006).
[22]Y. Xin, Z. H. Huang, L. Peng, and D. J. Wang, J. Appl. Phys. **105**, 086106 (2009).
[23]Y. Xin, Z. Huang, Z. Jiang, D. Li, L. Peng, J. Zhai, and D. Wang, Chem. Commun. (Cambridge) **2010**, 2316.
[24]D. Tu, S. Pagliara, A. Camposeo, L. Persano, R. Cingolani, and D. Pisignano, Nanoscale **2**, 2217 (2010).
[25]H. Liu, C. H. Reccius, and H. G. Craighead, Appl. Phys. Lett. **87**, 253106 (2005).
[26]N. J. Pinto, K. V. Carrasquillo, C. M. Rodd, and R. Agarwal, Appl. Phys. Lett. **94**, 083504 (2009).
[27]D. H. Reneker and I. Chun, Nanotechnology **7**, 216 (1996).
[28]S. Pagliara, A. Camposeo, A. Polini, R. Cingolani, and D. Pisignano, Lab Chip **9**, 2851 (2009).
[29]A. Camposeo, F. Di Benedetto, R. Stabile, R. Cingolani, and D. Pisignano, Appl. Phys. Lett. **90**, 143115 (2007).
[30]A. Camposeo, F. Di Benedetto, R. Stabile, A. A. R. Neves, R. Cingolani, and D. Pisignano, Small **5**, 562 (2009).
[31]Z. Bao, A. Dodabalapur, and A. J. Lovinger, Appl. Phys. Lett. **69**, 4108 (1996).
[32]Y.-Y. Noh, D.-Y. Kim, Y. Yoshida, K. Yase, B.-J. Jung, E. Lim, and H.-K. Shim, Appl. Phys. Lett. **86**, 043501 (2005).
[33]Y. Xu, P. R. Berger, J. N. Wilson, and U. H. F. Bunz, Appl. Phys. Lett. **85**, 4219 (2004).
[34]M. C. Hamilton, S. Martin, and J. Kanicki, IEEE Trans. Electron Devices **51**, 877 (2004).
[35]K. S. Narayan and N. Kumar, Appl. Phys. Lett. **79**, 1891 (2001).
[36]E. Frankevich, A. Zakhidov, K. Yoshino, Y. Maruyama, and K. Yakushi, Phys. Rev. B **53**, 4498 (1996).